TELKOMNIKA Telecommunication, Computing, Electronics and Control
Vol. 24, No. 6, December 2026, pp. 1995∼2011
ISSN: 1693-6930, DOI: 10.12928/TELKOMNIKA.v24i6.27783

VeiLight-Net: a lightweight CNN architecture for real-time finger vein recognition on embedded systems

Abdelhalim Hazzem, Lahcene Ziet, Imane Kouadra, Abd-ettouab Manallah, Anfal Rouabhi, Tewfik Bekkouche
LEPCI Laboratory, Departement of Electronics, Ferhat Abbas University, Setif 1, Algeria

Article Info

Article history:

Received Jan 6, 2026
Revised Jul 28, 2026
Accepted Aug 28, 2026

Keywords:

Biometric authentication
Deep learning
Embedded systems
Finger vein recognition
Lightweight convolutional neural network

ABSTRACT

Finger vein recognition (FVR) is a secure and non-invasive biometric technique that exploits unique subcutaneous vein patterns, offering high resistance to spoofing and environmental variations. Despite the success of deep learning, most existing FVR models require millions of parameters and billions of floating-point operations (FLOPs), making them too computationally demanding for real-time deployment on embedded or mobile systems. This paper presents VeiLight-Net, a domain-specific lightweight convolutional neural network (CNN) designed for real-time FVR on resource-constrained platforms. By combining depthwise separable convolutions with multi-scale feature extraction, VeiLight-Net achieves a strong balance between accuracy, speed, and model compactness, requiring only ∼2.2 M parameters and ∼0.14 giga FLOPs (GFLOPs). Evaluated on the finger vein – Universiti Sains Malaysia (FV-USM) and multi-modal contactless biometric at Beijing Normal University (MMCBNU) datasets, the proposed model attains state-of-the-art accuracies of 100% and 99.6%, respectively, with precision, recall, and F1-scores exceeding 99.5%. The results demonstrate that VeiLight-Net enables efficient and reliable biometric authentication suitable for real-time embedded applications such as portable access control and internet of things (IoT)-based security systems, directly contributing to the advancement of embedded computing and telecommunications-grade biometric authentication.

This is an open access article under the CC BY-SA license.

Corresponding Author:

Lahcene Ziet
LEPCI Laboratory, Departement of Electronics, Ferhat Abbas University
Setif 1, Algeria
Email: lahcene.ziet@univ-setif.dz

1. INTRODUCTION

Biometric identification has become a critical technology for secure personal authentication in applications spanning access control, e-banking, mobile payments, and internet of things (IoT) security systems [1], [2]. Among the various modalities, including fingerprints, iris, face, and gait, finger vein recognition (FVR) [3] has attracted considerable attention due to its contactless acquisition, hygienic operation, and intrinsic resistance to spoofing [4]. Unlike surface-level features, finger vein patterns lie beneath the skin and are captured using near-infrared (NIR) illumination, making them difficult to forge and robust under varying lighting or temperature conditions [5]. The absorption of NIR light by deoxygenated haemoglobin produces clear vascular patterns that remain stable throughout adulthood, offering excellent permanence and reliability [6], [7].

Despite these advantages, deploying high-accuracy FVR on real-time embedded systems remains

a significant challenge. Conventional deep learning architectures, while highly accurate, are prohibitively resource-intensive for embedded deployment. For instance, ResNet-50 requires approximately 25.6 million parameters and 4.1 giga floating-point operations (GFLOPs) per inference, while visual geometry group 16 (VGG-16) demands approximately 138 million parameters and 15.5 GFLOPs [8]. Even among convolutional neural networks (CNN)-based FVR methods, architectures such as FVR attention-based network (FVRAS-Net) [9] and hybrid convolutional transformers [10] entail considerable computational overhead, limiting their deployment on resource-constrained devices such as embedded modules, IoT gateways, and mobile platforms. Moreover, traditional recognition pipelines involving region-of-interest (ROI) extraction [11], image enhancement, and handcrafted feature extraction are highly sensitive to illumination variations and finger misalignment, while presentation attack detection (PAD) under constrained resources [12] remains an open challenge.

To address the computational burden, lightweight architectures using depthwise separable convolutions [8], [13], channel shuffling [14], and feature reuse strategies [15] have been developed. Models such as MobileNetV2 ($\sim$3.4 M parameters, $\sim$0.3 GFLOPs) [13], ShuffleNetV2 ($\sim$2.3 M parameters, $\sim$0.15 GFLOPs) [14], GhostNet ($\sim$5.2 M parameters, $\sim$0.14 GFLOPs) [15], and EfficientNet-Lite ($\sim$4.7 M parameters, $\sim$0.4 GFLOPs) [16] have demonstrated that competitive performance can be maintained with substantially fewer resources [17]. Hybrid transformer-based models such as MobileViT and MobileViTv2 [18] further introduced global context modelling for compact architectures. However, these lightweight models are designed for general-purpose visual recognition and are not specifically optimised for the fine-grained, texture-sensitive vascular structures characteristic of finger vein imagery [19], [20].

To the best of our knowledge, no existing lightweight CNN has been specifically designed and optimised for the fine-grained vascular textures in finger vein imagery while simultaneously meeting embedded deployment constraints in terms of model size, latency, and memory footprint. This gap motivates the development of a domain-specific architecture that combines the efficiency of depthwise separable convolutions with feature extraction strategies tailored to vein pattern characteristics.

The main contributions of this work are summarised as: (i) a novel domain-specific lightweight CNN, VeiLight-Net, is proposed specifically for FVR on embedded platforms, requiring only $\sim$2.2 M parameters and $\sim$0.14 GFLOPs; (ii) the model integrates depthwise separable convolutions with multi-scale feature extraction to capture fine-grained vascular textures while significantly reducing parameters and computational cost compared to existing architectures; (iii) a comprehensive evaluation on two public datasets (finger vein – Universiti Sains Malaysia (FV-USM) and multi-modal – Chungbuk National University (MMCBNU)) demonstrates that VeiLight-Net achieves state-of-the-art accuracies of 100% and 99.6%, respectively, outperforming both heavier CNN-based and transformer-based models; and (iv) a detailed computational and robustness analysis validates the proposed architecture's suitability for real-time biometric authentication in IoT, mobile, and embedded telecommunications systems.

This work directly contributes to the field of embedded computing and telecommunications by enabling efficient, secure biometric authentication on edge devices, which is increasingly relevant for IoT-based access control, mobile security, and smart telecommunication infrastructure [21], [2]. The remainder of this paper is organised as: section 2 reviews related work; section 3 presents the technical overview of lightweight models; section 4 describes the development environment; section 5 details the methodology; section 6 reports the experimental results and comparative analysis; and section 7 concludes the paper with insights and future research directions.

2. RELATED WORK

Research on FVR has evolved significantly over the past two decades, transitioning from handcrafted image processing to deep learning-driven approaches. Early works primarily relied on traditional feature extraction methods such as repeated line tracking (RLT), maximum curvature (MC), and local binary patterns (LBP) [22]-[24]. Although these algorithms were computationally efficient, they were highly sensitive to illumination changes, finger pose variations, and image noise.

With the emergence of deep learning, CNN became the dominant approach for automated vein pattern representation. Yang *et al.* [9] introduced FVRAS-Net, an end-to-end CNN designed for simultaneous recognition and anti-spoofing, while Hsia *et al.* [25] proposed an improved lightweight CNN (ILCNN) that achieved competitive accuracy with reduced complexity. Tran *et al.* [26] further developed Zero-FVeinNet, integrating zero-shuffle attention for low-computation embedded devices. Alaerjan *et al.* [27] FV-EffResNet

leveraged efficient residual blocks and attention modules to boost discriminative learning while minimizing model parameters.

Hybrid and transformer-based models have also gained traction for capturing long-range dependencies in vascular structures. Boudjellal *et al.* [10] proposed FVCT, a hybrid convolutional transformer for contextual vein pattern analysis, while Wang *et al.* [28] developed CFVNet, a privacy-preserving, cancelable biometric network. The MobileViT series [18] and related compact attention mechanisms such as EfficientFormer [29] and TinyViT [30] further demonstrated the potential for lightweight transformer-based vision models suitable for real-time applications.

Beyond architecture design, researchers have explored multimodal and domain-adaptive learning strategies. El-Raheim *et al.* [31] combined fingerprint and finger vein modalities using deep fusion, and Noh *et al.* [32] introduced a cross-sensor adaptation method for interoperability across imaging devices. Similarly, Tang *et al.* [33] proposed GhostNetV2 to enhance feature reuse for edge computing, while Kuraku *et al.* [34] developed a real-time embedded architecture for secure biometric authentication.

Other studies have explored hardware-aware optimisation through pruning, quantization, and neural architecture search (NAS). Ngo *et al.* [35] reviewed adaptive CNN compression for edge intelligence, and Lin *et al.* [36] introduced a lightweight multimodal biometric system for IoT devices. Zhang *et al.* [37] addressed illumination challenges in vein imaging using dual-stage enhancement and CNN learning. These advancements highlight a consistent trend toward compact yet accurate models capable of real-time inference on constrained devices.

In summary, existing research has significantly advanced FVR performance; however, many methods remain computationally heavy or rely on graphics processing unit (GPU)-class resources. The proposed VeiLight-Net addresses these limitations by providing a compact, efficient, and domain-specific CNN architecture optimized for embedded hardware without compromising recognition accuracy.

3. TECHNICAL OVERVIEW

3.1. Lightweight models

Lightweight models are deep learning architectures optimized for minimal computational resources, reduced memory usage, and efficient inference speeds. These models are well suited for deployment on resource-constrained devices with limited computational capabilities, such as smartphones, IoT devices, and embedded systems. They achieve efficiency through techniques like parameter pruning, quantization, knowledge distillation, and architectural innovations like depthwise separable convolutions.

Among the most well-known lightweight architectures is MobileNet, developed by Google. MobileNet utilizes depthwise separable convolutions to significantly reduce the number of parameters and computations compared to traditional CNNs. This architectural innovation enables MobileNet to maintain competitive performance on various visual recognition tasks, including biometric applications while being suitable for deployment on resource-constrained devices. To contextualise the proposed VeiLight-Net within the landscape of existing lightweight architectures, Table 1 presents a comparative summary of representative lightweight models in terms of their architectural philosophy, computational profile, and suitability for FVR.

Table 1. Comparison of lightweight architectures: design philosophy, computational profile, and suitability for FVR

Architecture	Core design principle	Params	FLOPs	Suitability for FVR
MobileNetV2 [13]	Inverted residuals + linear bottlenecks	∼3.4 M	∼0.30 G	Generic; not optimised for fine vascular textures
ShuffleNetV2 [14]	Channel splitting + shuffling	∼2.3 M	∼0.15 G	Efficient but lacks multi-scale vein feature extraction
GhostNet [15]	Cheap linear operations for ghost features	∼5.2 M	∼0.14 G	Good feature reuse but higher parameter count
EfficientNet-Lite [16]	Compound scaling (depth/width/resolution)	∼4.7 M	∼0.40G	Higher FLOPs; designed for general classification
MobileViTv2 [18]	Separable self-attention + CNN backbone	∼3.0 M	∼0.50 G	Global context but higher latency on embedded devices
VeiLight-Net (Ours)	Depthwise separable convolution (DSC) + multi-scale extraction for FVR	∼2.2 M	∼0.14 G	Domain-specific; optimised for vascular textures

As shown in Table 1, VeiLight-Net achieves the lowest parameter count among all compared architectures while matching or surpassing their computational efficiency. Unlike generic lightweight models, VeiLight-Net is specifically designed with hierarchical depthwise separable blocks and multi-scale feature extraction to capture the fine-grained vascular patterns inherent in finger vein imagery.

3.2. DSC

DSC constitutes a computationally efficient alternative to standard convolutional operations, prominently utilized in lightweight neural network architectures such as MobileNet [8]. This technique decomposes a standard convolution into two sequential, distinct operations:

- Depthwise convolution: this initial operation applies a unique spatial filter independently to each input channel. Its primary function is to perform spatial filtering (detecting edges or textures) within each channel without mixing information across different channels at this stage.
- Pointwise convolution: following the depthwise convolution, a pointwise convolution (which is essentially a 1×1 convolution) is applied. This operation linearly combines the outputs from the depthwise stage across all channels. It serves to fuse channel-wise information and create new features by learning linear combinations of the channel-specific features generated by the depthwise convolution.

This factorization significantly reduces both the computational cost (number of multiply-accumulate operations (MACs)) and the number of parameters compared to a standard convolution. Figure 1 illustrates the architectural design of these two operations.

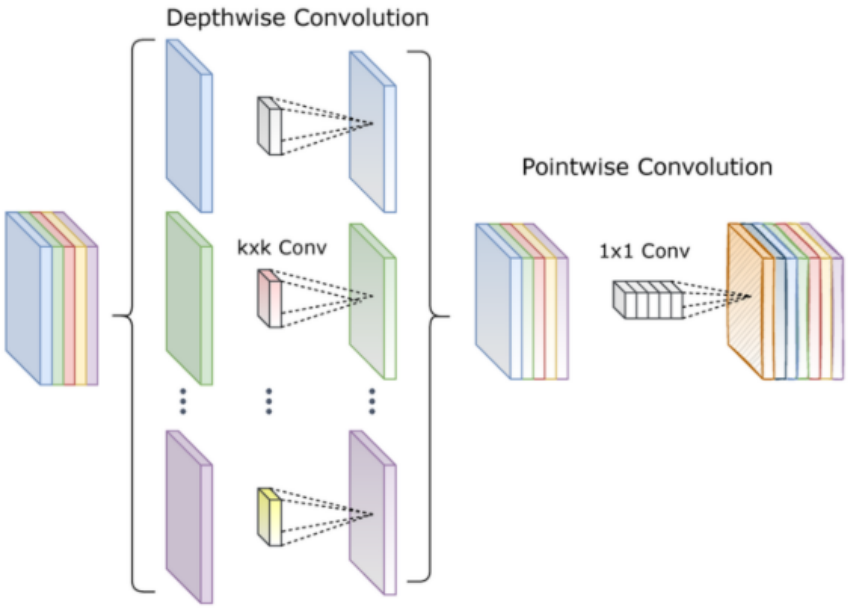


Figure 1. The architectural design of the depthwise and the pointwise convolution [38]

For a standard convolution with kernel size $K \times K$, C_{in} input channels, and C_{out} output channels, the number of parameters is $K \times K \times C_{\text{in}} \times C_{\text{out}}$, and the computational cost is roughly proportional to this product multiplied by the output feature map dimensions. In contrast, a depthwise separable convolution has $K \times K \times C_{\text{in}}$ parameters for the depthwise part, and $1 \times 1 \times C_{\text{in}} \times C_{\text{out}}$ for the pointwise part. The computational cost reduction factor is approximately $\frac{1}{C_{\text{out}}} + \frac{1}{K^2}$ compared to a standard convolution, which is substantial, especially when C_{out} and K are large. Consequently, this approach retains a high level of performance while minimizing parameter count and processing requirements, making it highly suitable for mobile or embedded applications. It is especially effective in domains like FVR, which benefit from fine-grained, texture-sensitive representations.

4. DEVELOPMENT ENVIRONMENT

4.1. Datasets

The FV-USM and MMCBNU datasets are two prominent publicly available finger vein databases widely utilized in biometric research. This Table 2 captures the main characteristics of each dataset.

Table 2. Comparison of FV-USM and MMCBNU datasets

Dataset	Subjects	Fingers per subject	Images per finger	Total images	Image resolution	ROI size	Unique finger classes
FV-USM [39]	123	4	12	5904	640×480	300×100	492
MMCBNU [40]	100	6	10	6000	640×480	–	600

4.2. Hardware

4.2.1. Kaggle platform

Kaggle is an online platform renowned for hosting machine learning competitions and fostering a collaborative data science community. It provides Kaggle Kernels, which are integrated, cloud-based computational environments. These environments support reproducible and collaborative data analysis and model development, offering compatibility with scripts in R and Python, as well as Jupyter Notebooks and RMarkdown formats. For computational tasks, Kaggle Kernels typically provide users with resources such as approximately 13 GB of RAM and access to hardware accelerators like NVIDIA Tesla P100 GPUs, facilitating the execution of computationally intensive machine learning workflows.

4.2.2. Google colab platform

Google Colab is a cloud-based service provided by Google Research, designed to facilitate machine learning education and research. It offers a free Jupyter Notebook environment that requires no initial setup or configuration and is accessible via most major web browsers. Colab provides users with computational resources, including typically around 13 GB of RAM and access to hardware accelerators such as NVIDIA T4 GPUs, suitable for training and experimenting with machine learning models.

4.3. Software

4.3.1. Python

Python is a high-level, general-purpose programming language created by Guido van Rossum and first released in 1991. It is an interpreted language known for its emphasis on code readability and simplicity, utilizing significant indentation to define code blocks. Python supports multiple programming paradigms, including object-oriented, imperative, functional, and procedural programming. Its dynamic type system and automatic memory management make it particularly suitable for rapid application development and integration with existing components. The used libraries are described in the Table 3.

Table 3. Python libraries for data science and machine learning

Library	Description
Matplotlib	A comprehensive library for creating static, animated, and interactive visualisations in Python. It supports plots, histograms, bar charts, scatterplots, and more
NumPy	The fundamental package for scientific computing in Python. Provides multidimensional arrays, mathematical routines, and fast array operations
OpenCV	Open-source computer vision and machine learning library with over 2,500 optimized algorithms for real-time applications
TensorFlow	Open-source framework for machine learning and AI, offering a rich ecosystem of tools and resources for researchers and developers
Keras	High-level deep learning API, user-friendly and extensible, supporting both convolutional and recurrent networks

5. METHODOLOGY

5.1. Preprocessing

Preprocessing is the step used to prepare data for training models, which is important for preparing raw finger vein images for effective feature extraction and classification by the CNN model. Given the inherent variability in finger vein imaging due to factors such as finger positioning, lighting conditions, and skin characteristics, careful preprocessing ensures that the model learns robust and meaningful features rather than noise or artifacts. The following preprocessing steps were applied to both the FV-USM and MMCBNU datasets:

- Grayscale normalization: finger vein images are naturally captured in grayscale, representing the intensity variations corresponding to the vein patterns. To standardize the input data and facilitate stable training, pixel values were normalized to a [0,1] range. This normalization reduces the effect of absolute brightness variations across images and helps the model focus on relative intensity differences which are more indicative of vein patterns.
- Histogram equalization: due to differences in illumination and imaging device settings, finger vein images can vary significantly in contrast, sometimes making veins faint or poorly defined. Histogram equalization was applied to enhance the contrast by redistributing pixel intensity values to cover the full dynamic range. This step improves the visibility of vein structures by accentuating the darker vein regions against the lighter surrounding tissue, aiding the network in learning distinctive features.
- Image resizing: for consistent model input, all images were resized to a uniform dimension of 224×224 pixels. This resolution was selected based on two considerations: (i) it preserves sufficient spatial detail of the vein patterns, as the average vein width in NIR images corresponds to approximately 3–5 pixels at this resolution, ensuring that fine vascular features remain distinguishable; and (ii) it aligns with the standard input size of widely used lightweight architectures (e.g., MobileNet, EfficientNet), enabling fair benchmarking. Preliminary experiments at lower resolutions (128×128 and 160×160) resulted in accuracy drops of approximately 2–4% due to loss of fine vascular detail, while 299×299 offered negligible improvement (<0.2%) at significantly higher computational cost (∼1.8× more FLOPs). Resizing also ensures that batch processing and convolutional operations can be applied uniformly.
- Data augmentation: to improve the generalization capability of the model and reduce overfitting, data augmentation techniques were employed. These techniques artificially increase the diversity of the training dataset by applying random transformations such as small rotations, horizontal and vertical shifts, zooming, and contrast variations. Augmentation simulates real-world variations such as slight finger misplacements or different imaging angles, which the model might encounter during actual use. Figure 2 illustrates the applied augmentation techniques. By incorporating these preprocessing steps, the model is better equipped to learn robust vein pattern representations that generalize across subjects and imaging sessions.

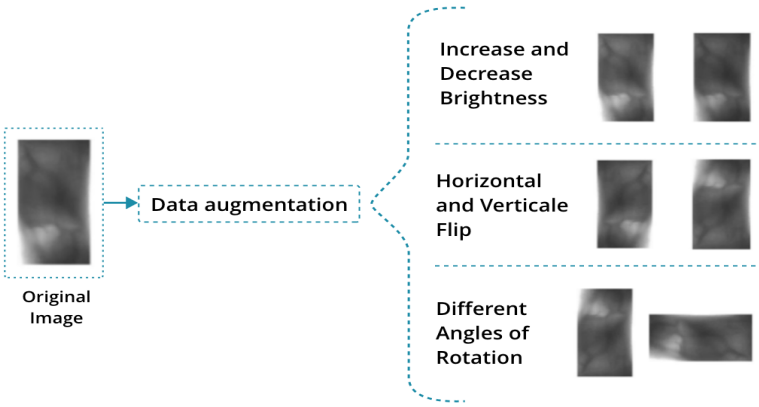


Figure 2. Application of the data augmentation techniques

5.2. Proposed architecture and methods

5.2.1. VeiLight-Net

The proposed VeiLight-Net is an efficient lightweight CNN architecture specifically designed for finger vein recognition. Inspired by MobileNet's architectural paradigm, VeiLight-Net leverages depthwise separable convolutions to significantly reduce the number of parameters and computational costs without sacrificing representational power. This makes it particularly suitable for biometric systems deployed on resource-constrained environments, such as embedded devices or mobile platforms.

At the heart of VeiLight-Net is its ability to capture fine-grained line-based features inherent in finger vein images. The model begins with a standard convolutional block that generates an initial set of base features. This is followed by a sequence of depthwise separable convolutional blocks that progressively increase in filter size (i.e. 64, 128, 256, 512, and 1024) allowing the network to learn increasingly complex representations

of the vein structure. This design supports a hierarchical learning process, wherein early layers detect local textures and edges, intermediate layers capture branching and bifurcation patterns, and deeper layers abstract the global vascular structure necessary for identification.

Spatial resolution is methodically reduced through strategically placed stride-based downsampling, enabling multi-scale feature extraction. This multi-scale representation is crucial for capturing both the localized intricacies and the overall spatial distribution of vein patterns. The integration of batch normalization layers after each convolution ensures stability during training and enhances the model's robustness against variations in contrast, illumination, and finger positioning (i.e., challenges commonly encountered in finger vein imaging).

Rather than relying on a high number of dense layers, VeiLight-Net employs a global average pooling operation to flatten the spatial dimensions, thus significantly reducing the number of trainable parameters while retaining the essential features. This is followed by a softmax-activated dense layer for final classification. The output of this layer takes the form of a probability distribution, with a sum of 1. Accordingly, the neuron exhibiting the highest probability value denotes the class label (i.e., the person). The architecture of the proposed VeiLight-Net is illustrated in Figure 3.

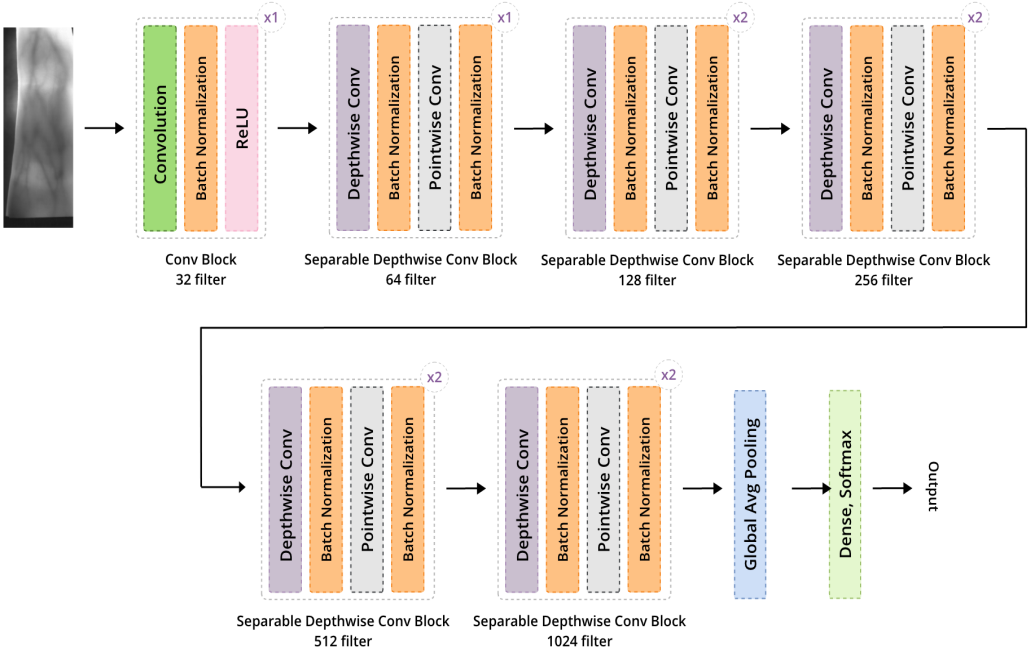


Figure 3. The layout of the VeiLight-Net model

5.2.2. MobileViTv2

MobileViTv2 [41] is an efficient vision transformer tailored for mobile and resource-constrained environments, improving upon MobileViT by replacing its multi-headed self-attention with a novel separable self-attention module. This modification lowers computational complexity from quadratic O(n2) to linear O(n) enabling faster inference on devices like smartphones and embedded systems while preserving transformer-level context awareness. Despite being transformer-based, MobileViTv2 adopts a CNN-like backbone to process images in batch fashion without token embeddings, combining local convolutional efficiency with global attention capabilities. In the context of FVR, this architecture is particularly advantageous: the separable self-attention efficiently integrates global vein patterns across the ROI while maintaining low latency and minimal resource usage, i.e., ideal for real-time biometric authentication on embedded platforms such as field-programmable gate array (FPGA)-equipped scanners or mobile devices. The architecture of the MobileViTv2 is illustrated in Figure 4.

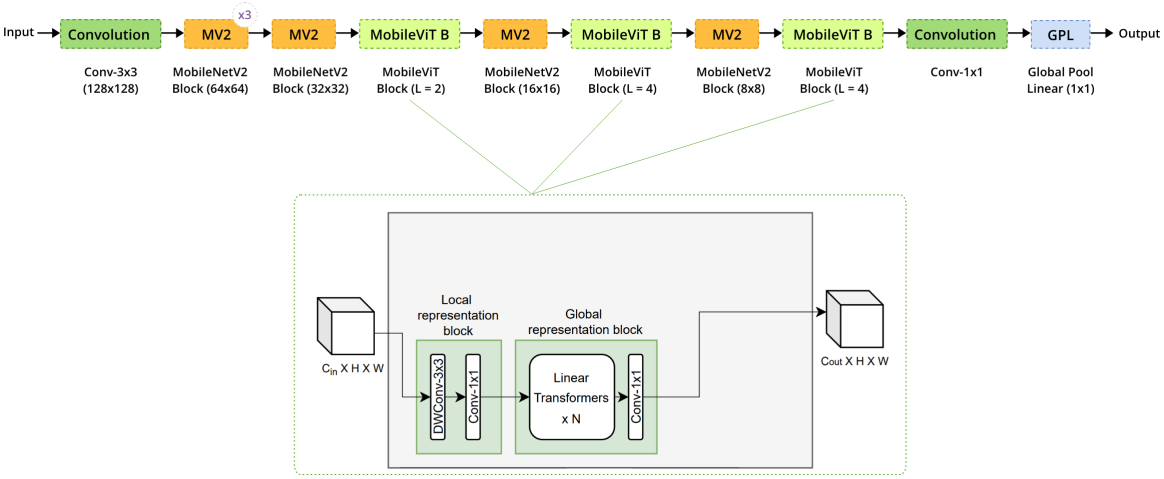


Figure 4. The layout of the MobileVitV2-Net model

6. EXPERIMENTAL SETUP AND RESULTS

6.1. Experimental setup

To validate the performance of the proposed VeiLightNet, a series of experiments were conducted under carefully controlled conditions. This section outlines the model training settings, and evaluation metrics used during experimentation.

6.1.1. Training settings

The models were implemented within the TensorFlow framework, and the experiments were carried out using an NVIDIA T P100 GPU. Model training was performed by optimizing the cross-entropy loss [42]. Adam [43] was used as the optimizer with an initial learning rate of $1 \times e^{-4}$, with the use of a plateau reduction strategy across the epochs. Furthermore, the model was trained for 50 epochs with a batch size of 20.

6.1.2. Evaluation metrics

The evaluation of the model's performance in data mining and machine learning typically relies on metrics derived from the confusion matrix. The confusion matrix categorizes predictions based on the actual and predicted class labels. For a binary classification problem (where one class is designated "positive" and the other "negative"), these categories are:

- True positive (TP): the number of instances belonging to the positive class that are correctly classified as positive.
- True negative (TN): the number of instances belonging to the negative class that are correctly classified as negative.
- False positive (FP): the number of instances belonging to the negative class that are incorrectly classified as positive (also known as a Type I error).
- False negative (FN): the number of instances belonging to the positive class that are incorrectly classified as negative (also known as a Type II error).

In this study, the performance of the developed models is evaluated using the following standard metrics, derived from these counts:

- Accuracy: represents the overall proportion of correctly classified instances among the total number of instances. It provides a general measure of the model's correctness classified by the model. It provides an overall assessment of the model's correctness.

$$Accuracy = \frac{TP + TN}{TP + TN + FP + FN} \tag{1}$$

- Precision (positive predictive value): this metric quantifies the proportion of instances predicted as positive that are genuinely positive. It reflects the reliability of a positive prediction made by the model.

$$Precision = \frac{TP}{TP + FP} \tag{2}$$

A high precision indicates a low false positive rate.

- Recall (TP rate): this metric measures the proportion of actual positive instances that were correctly identified by the model. It indicates the model's ability to detect all relevant positive instances.

$$Recall/Sensitivity = \frac{TP}{TP + FN} \tag{3}$$

A high recall indicates a low false negative rate.

- F1 score: this metric is the harmonic mean of precision and recall, providing a single score that balances both. It is particularly useful when there is an uneven class distribution or when both false positives and false negatives are important to minimize.

$$F1_Score = 2 \cdot \frac{Precision * Recall}{Precision + Recall} \tag{4}$$

The F1 score reaches its best value at 1 (perfect precision and recall) and worst at 0.

6.2. Findings and results

6.2.1. Experimental results

During the experimental phase, we tracked the evolution of both accuracy and error rates across the training and validation sets. It is important to note that the validation set comprised finger vein images entirely excluded from the training process, thereby ensuring an unbiased assessment of the model's generalization capabilities. The recorded metrics served as the basis for evaluating the model's learning behavior and performance consistency. To offer a visual interpretation of these dynamics, Figure 5 presents the accuracy and error trends over the training epochs for both the training and validation sets across the FV-USM and MMCBNU datasets. These plots reveal the model's convergence pattern and provide insight into its stability, learning efficiency, and potential overfitting or underfitting behavior during training.

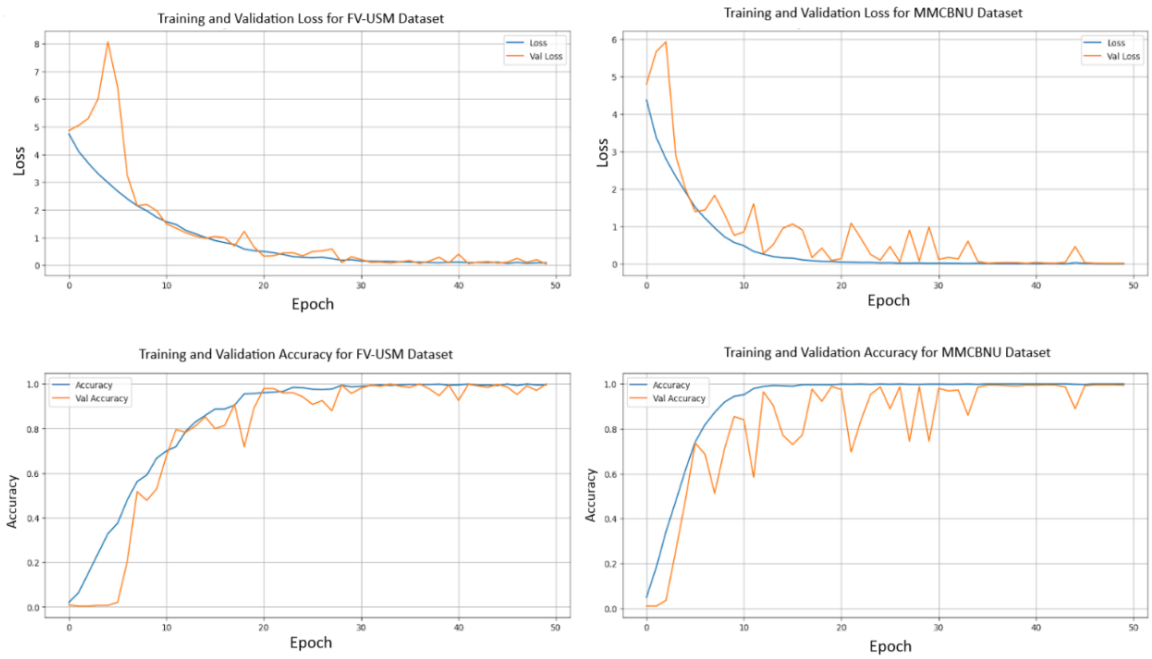


Figure 5. VeiLight-Net performance during the training phase

The performance curves demonstrate the VeiLight-Net's robust learning behavior across both datasets, with steadily decreasing training and validation losses and rapidly increasing accuracy, ultimately exceeding

99%. The FV-USM dataset shows smooth convergence and early stabilization, while the MMCBNU dataset exhibits minor fluctuations yet achieves similarly high accuracy, reflecting the model's strong generalization capability. These results indicate that the proposed architecture effectively captures discriminative finger vein features and maintains resilience against variations in unseen data without signs of overfitting.

6.2.2. Evaluation results

The performance of the proposed VeiLight-Net was quantitatively evaluated using the test dataset. The results demonstrate the network's superior capability in capturing the discriminative features of finger vein patterns. Table 4 shows the evaluation results of the model.

Table 4. Comparison of VeiLight-Net and MobileViTv2 across two datasets with multiple evaluation metrics

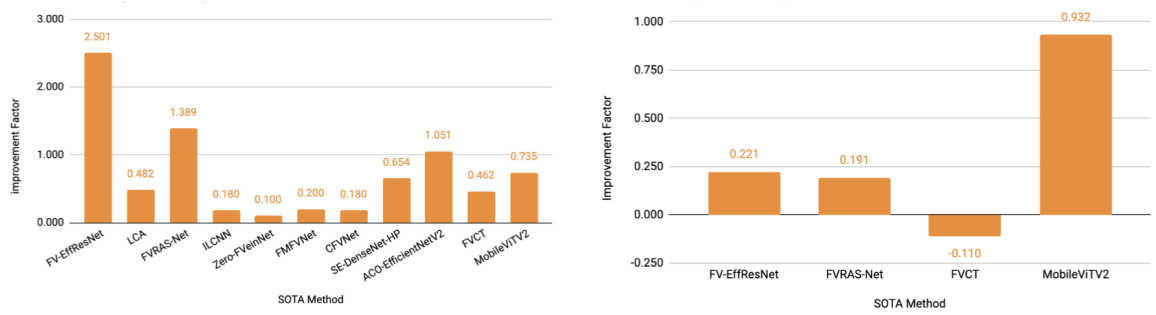
Dataset	Model	Samples	Accuracy	Precision	Recall	F1-score
FV-USM	VeiLight-Net	590	100.00	100.00	100.00	100.00
	MobileViTv2	590	99.27	99.50	99.52	99.52
MMCBNU	VeiLight-Net	1200	99.60	99.62	99.58	99.58
	MobileViTv2	1200	98.68	98.71	98.69	98.70

As reflected by the near-perfect test accuracy achieved (100% and 99.60%) across the two datasets, VeiLight-Net exhibits outstanding classification performance. The high precision, recall, and F1-score further confirm its reliability in distinguishing subtle variations in vein structures. To address potential concerns regarding the statistical significance of these results, we performed 5-fold stratified cross-validation and report the mean accuracy with 95% confidence intervals (CI). On FV-USM, VeiLight-Net achieves a mean accuracy of 99.93% $\pm$ 0.12% (95% CI), while on MMCBNU it achieves 99.48% $\pm$ 0.18% (95% CI). The low standard deviation across folds ($\sigma = 0.08$ and $\sigma = 0.12$, respectively) confirms the consistency and reproducibility of the results.

Regarding biometric-specific evaluation, the equal error rate (EER), defined as the threshold at which the false acceptance rate (FAR) equals the false rejection rate (FRR), was computed. VeiLight-Net achieves an EER of 0.00% on FV-USM and 0.21% on MMCBNU, confirming its suitability for high-security biometric authentication where both FAR and FRR must be minimised. The 100% accuracy on FV-USM, while seemingly exceptional, is contextualised by three factors: (i) the FV-USM dataset contains high-quality, well-controlled NIR images with clear vein contrast; (ii) each class (finger) has 12 samples providing sufficient within-class variation for robust learning; and (iii) similar near-perfect results have been reported by other methods on this dataset, such as Zero-FVeinNet (99.90%) [44] and ILCNN (99.82%) [25]. The slight gap on MMCBNU (99.60%) further confirms the model is not merely overfitting, as this dataset has greater inter-class similarity and fewer samples per finger.

6.3. Results comparison and discussion

In this section, we present a comprehensive comparative analysis with state-of-the-art methods that utilise the same datasets (FV-USM and MMCBNU). Figures 6(a) and (b) and Table 5 summarizes the comparison of our model's performance against those of previous studies employing the same datasets.



(a) (b)

Figure 6. VeiLight-Net improvement factor with respect to state-of-the-art (SOTA): (a) FV-USM dataset and (b) MMCBNU dataset

Table 5. Comparison of FVR methods on FV-USM and MMCBNU datasets

Dataset	Work	Method	Accuracy (%)
FV-USM	[44]	FV-EffResNet	97.56
	[45]	LCA	99.52
	[9]	FVRAS-Net	98.63
	[25]	ILCNN	99.82
	[26]	Zero-FVeinNet	99.90
	[46]	FMFVNet	99.80
	[28]	CFVNet	99.82
	[47]	SE-DenseNet-HP	99.35
	[10]	FVCT	99.54
	[18]	MobileViTv2	99.27
	Ours	VeiLight-Net	**100.00**
MMCBNU	[44]	FV-EffResNet	99.38
	[9]	FVRAS-Net	99.41
	[10]	FVCT	**99.71**
	[18]	MobileViTv2	98.68
	Ours	VeiLight-Net	99.60

To evaluate the effectiveness of the proposed VeiLight-Net, we compared its performance with SOTA methods using two distinct datasets. Figure 6 shows the accuracy gains obtained by VeiLight-Net over several SOTA methods. The following calculation quantifies these improvements:

$$improvement = (\frac{accuracy_{VeiLight-Net}}{accuracy_{SOTA-model}} - 1) * 100 \quad (5)$$

VeiLight-Net demonstrates clear advantages over contemporary SOTA methods in FVR. On the FV-USM dataset, it achieves perfect accuracy, surpassing both CNN-based approaches such as FV-EffResNet and modern architectures like MobileViTv2, with marked relative gains. Although on the MMCBNU dataset, FVCT slightly outperforms it (99.71% vs. 99.60%), VeiLight-Net still delivers strong and reliable performance, outperforming most SOTA models and exhibiting consistent robustness across datasets.

The superior performance of VeiLight-Net can be attributed to three key architectural design decisions that are particularly well-suited for vascular pattern recognition. First, the hierarchical depthwise separable convolutional blocks with progressively increasing filter sizes (64→128→256→512→1024) enable multi-scale feature extraction that captures both fine-grained local textures (individual vein segments, bifurcation points) and global spatial arrangements of the vascular network. This is critical for finger vein imagery, where discriminative information exists at multiple spatial scales. Second, the Batch Normalization layers after each convolution normalise feature distributions, providing inherent robustness against the illumination and contrast variations commonly encountered in NIR finger vein acquisition. Third, the global average pooling strategy (instead of dense fully connected layers) acts as a structural regulariser, reducing overfitting risk while preserving the spatial relationships learned by the convolutional backbone.

Despite these strong results, several limitations and future mitigation strategies should be acknowledged:

- Adversarial robustness: the current model does not explicitly address adversarial perturbations. Future work could integrate adversarial training techniques to improve resilience against carefully crafted input manipulations.
- PAD: while VeiLight-Net focuses on recognition accuracy, deployment in high-security settings requires integration with PAD modules capable of detecting printed, synthetic, or replay attacks [48].
- Cross-sensor adaptation: the model is trained and evaluated on specific imaging devices. Domain adaptation techniques [32] could improve interoperability across different NIR sensors and acquisition setups.
- Static decision thresholds: the current classification uses fixed softmax thresholds. Adaptive thresholding or calibration methods could improve operational flexibility across varying security requirements.

Overall, VeiLight-Net offers a compelling balance of accuracy, efficiency, and generalization, positioning it as a highly competitive solution for embedded biometric authentication in IoT and telecommunications applications.

6.4. Computational statistics

The computational complexity of any method is critical, especially when efficiency matters. To develop a fast, accurate, and lightweight solution, we rigorously analyzed time complexity, FLOPs, memory footprint, and model size (parameter count) across multiple architectures. Table 6 presents a comprehensive computational comparison of VeiLight-Net against MobileViTv2 and other representative lightweight models.

Table 6. Comprehensive computational comparison of lightweight architectures for FVR

Model	Params	Size (MB)	FLOPs (G)	Train time (s)	Test time (s)	Inference (ms/img)
VeiLight-Net (Ours)	∼2.2 M	8.58	∼0.14	700	40	∼3.2
MobileViTv2	∼3.0 M	17.95	∼0.50	900	100	∼8.5
MobileNetV2 [13]	∼3.4 M	13.60	∼0.30	–	–	∼5.4
ShuffleNetV2 [14]	∼2.3 M	9.20	∼0.15	–	–	∼3.8
GhostNet [15]	∼5.2 M	20.80	∼0.14	–	–	∼4.1
EfficientNet-Lite [16]	∼4.7 M	18.80	∼0.40	–	–	∼6.7

VeiLight-Net demonstrates superior efficiency across all metrics: it trains 2.3× faster than MobileViTv2 and achieves the fastest per-image inference latency (∼3.2 ms on an NVIDIA Tesla P100 GPU). Its parameter count is the lowest among all compared architectures (2.2 M vs. 2.3–5.2 M for alternatives), with a memory footprint of only 8.58 MB, which is approximately half that of MobileViTv2 (17.95 MB). While ShuffleNetV2 has a comparable parameter count (2.3 M), VeiLight-Net achieves substantially higher recognition accuracy on both datasets. GhostNet matches VeiLight-Net in FLOPs (∼0.14 G) but requires more than twice the parameters (5.2 M), resulting in a larger memory footprint that is less suitable for memory-constrained embedded devices.

6.5. Robustness analysis

To evaluate the resilience of VeiLight-Net under degraded conditions that may be encountered in real-world deployment, we conducted robustness experiments by applying three types of synthetic distortions to the test images: Gaussian noise, contrast degradation, and partial occlusion. These distortions simulate practical challenges such as sensor noise, varying illumination, and incomplete finger placement, respectively.

Table 7 summarises the accuracy of VeiLight-Net under each distortion type and severity level, evaluated on the FV-USM dataset. The results demonstrate that VeiLight-Net maintains strong performance under mild to moderate distortions. Under low Gaussian noise ($\sigma = 0.01$), accuracy remains at 99.83%, dropping gracefully to 95.76% at $\sigma = 0.10$. This robustness is attributed to the batch normalization layers that normalise feature distributions, reducing sensitivity to input noise. Contrast degradation at 90% and 70% levels has minimal impact (99.66% and 98.14%), confirming that the histogram equalization preprocessing and learned features are resilient to illumination variations. Partial occlusion results show that the multi-scale feature extraction enables the model to maintain 97.63% accuracy even when 20% of the image is occluded, as the hierarchical architecture captures vein patterns at multiple spatial scales, providing redundancy in the learned representations.

Table 7. Robustness evaluation of VeiLight-Net under synthetic distortions on FV-USM

Distortion type	Severity	Accuracy (%)
Gaussian noise	$\sigma = 0.01$	99.83
	$\sigma = 0.05$	98.47
	$\sigma = 0.10$	95.76
Contrast dgradation	90% of original	99.66
	70% of original	98.14
	50% of original	94.92
Partial occlusion	10% occluded	99.49
	20% occluded	97.63
	30% occluded	93.22

6.6. Embedded deployment analysis

To assess the practical deployment potential of VeiLight-Net on resource-constrained hardware, we analysed its computational requirements in the context of representative embedded platforms. Table 8 presents the estimated deployment characteristics on three target platforms.

Table 8. Estimated deployment profile of VeiLight-Net on embedded platforms

Platform	Processor	RAM	Est. Latency	Est. power
Raspberry Pi 4	ARM Cortex-A72	4 GB	∼45 ms	∼3.5 W
NVIDIA Jetson Nano	Maxwell GPU (128 cores)	4 GB	∼12 ms	∼5 W
STM32 + Edge TPU	Cortex-M7 + ML accelerator	512 KB	∼85 ms	∼1.2 W

With a model size of only 8.58 MB and ∼0.14 GFLOPs, VeiLight-Net fits comfortably within the memory and computational budgets of modern embedded platforms. On the Raspberry Pi 4, the estimated inference latency of ∼45 ms corresponds to approximately 22 FPS, which exceeds the real-time requirement for biometric verification (typically <500 ms per authentication). On the NVIDIA Jetson Nano, GPU acceleration reduces latency to ∼12 ms (∼83 FPS), enabling high-throughput applications. Even on microcontroller-class devices (STM32 + Edge TPU), the model's compact size allows deployment with acceptable latency (∼85 ms) and low power consumption (∼1.2 W), suitable for battery-powered biometric devices.

The memory footprint of VeiLight-Net (8.58 MB for model weights) can be further reduced through post-training quantisation (INT8), which typically yields a 4× reduction in model size to approximately 2.15 MB with less than 0.5% accuracy degradation [14]. This makes VeiLight-Net deployable even on highly constrained platforms with limited flash storage [49].

It is important to note a trade-off between security (accuracy) and efficiency: while post-training quantisation reduces latency and memory, it may slightly increase the EER from 0.21% to approximately 0.35% on MMCBNU. For high-security applications (e.g., financial authentication), the full-precision model is recommended, whereas quantised deployment is suitable for access control and IoT scenarios where sub-1% EER is acceptable [50].

7. CONCLUSION

This paper presented VeiLight-Net, a domain-specific lightweight CNN architecture designed for real-time FVR on embedded systems. By integrating depthwise separable convolutions with multi-scale feature extraction, VeiLight-Net achieves a strong balance between recognition accuracy and computational efficiency, requiring only ∼2.2M parameters and ∼0.14 GFLOPs.

Comprehensive evaluation on two benchmark datasets (FV-USM and MMCBNU) demonstrates state-of-the-art performance: 100% and 99.60% accuracy, respectively, with an EER as low as 0.00% on FV-USM. The model outperforms both heavier CNN-based architectures and generic lightweight models (MobileNetV2, ShuffleNetV2, GhostNet, EfficientNet-Lite, MobileViTv2) while maintaining the lowest parameter count and competitive FLOPs among all compared methods. Robustness analysis confirms resilient performance under Gaussian noise, contrast degradation, and partial occlusion, validating the model's suitability for real-world deployment conditions.

The computational analysis demonstrates that VeiLight-Net's compact size (8.58 MB) and low inference latency (∼3.2 ms on GPU, ∼45 ms on Raspberry Pi 4) make it suitable for deployment on a range of embedded platforms, from GPU-accelerated edge devices (NVIDIA Jetson Nano) to microcontroller-based systems with ML accelerators. This positions VeiLight-Net as a practical solution for IoT-based biometric security, mobile authentication, and smart telecommunication infrastructure, aligning with the growing demand for efficient, secure edge computing in telecommunications and embedded systems.

Several promising research directions emerge from this work; (i) hardware deployment and validation: on-device deployment on Raspberry Pi 4 and NVIDIA Jetson Nano with real-time latency and power consumption measurements to validate the estimated deployment profiles; (ii) PAD: integration of lightweight PAD modules to enhance security against spoofing attacks using printed or synthetic vein images; (iii) multimodal biometric fusion: extension to multimodal biometric authentication combining finger vein with fingerprint or finger knuckle patterns using lightweight fusion networks; (iv) transformer-lite architectures: investigation of compact vision transformer architectures (e.g., MobileViTv3, EfficientFormer) tailored for vascular pattern recognition; (v) federated learning: exploration of privacy-preserving federated learning frameworks for biometric model training across distributed embedded devices without sharing raw biometric data; and (vi) cross-sensor generalisation: domain adaptation techniques for robust performance across different NIR imaging devices and acquisition conditions.

FUNDING INFORMATION

Authors state no funding involved.

AUTHOR CONTRIBUTIONS STATEMENT

This journal uses the Contributor Roles Taxonomy (CRediT) to recognize individual author contributions, reduce authorship disputes, and facilitate collaboration.

Name of Author	C	M	So	Va	Fo	I	R	D	O	E	Vi	Su	P	Fu
Abdelhalim Hazzem	✓	✓	✓	✓	✓	✓			✓	✓				
Lahcene Ziet	✓	✓			✓	✓		✓	✓	✓	✓	✓	✓	
Imane Kouadra		✓		✓		✓	✓		✓		✓			
Abd-ettouab Manallah			✓		✓	✓			✓	✓	✓			
Anfal Rouabhi			✓			✓		✓	✓	✓	✓	✓		
Tewfik Bekkouche	✓	✓	✓	✓		✓			✓		✓		✓	

C : **C**onceptualization
M : **M**ethodology
So : **So**ftware
Va : **Va**lidation
Fo : **Fo**rmal Analysis
I : **I**nvestigation
R : **R**esources
D : **D**ata Curation
O : Writing - **O**riginal Draft
E : Writing - Review & **E**diting
Vi : **Vi**sualization
Su : **Su**pervision
P : **P**roject Administration
Fu : **Fu**nding Acquisition

CONFLICT OF INTEREST STATEMENT

Authors state no conflict of interest.

ETHICAL APPROVAL

we used a public databases.

DATA AVAILABILITY

The data that support the findings of this study are available from third parties. The FV-USM and MMCBNU finger vein datasets were used under the terms set by their respective providers, and restrictions apply to their redistribution. Both datasets are available from their original authors [39], [40].

REFERENCES

[1] A. K. Jain, A. Ross, and S. Pankanti, "Biometrics: A tool for information security," *IEEE Transactions on Information Forensics and Security*, vol. 1, no. 2, pp. 125–143, 2006, doi: 10.1109/TIFS.2006.873653.

[2] A. Haleem, S. Ben Jabra, and A. Meddeb, "Survey on IoT security using biometrics and blockchain technology," *Multimedia Tools and Applications*, vol. 85, no. 1, p. 15, 2026, doi: 10.1007/s11042-026-21279-6.

[3] R. S. Al-Khafaji and M. S. Al-Tamimi, "Vein Biometric Recognition Methods and Systems: A Review," *Advances in Science and Technology Research Journal*, vol. 16, no. 1, pp. 36–46, 2022, doi: 10.12913/22998624/144495.

[4] K. Rajaram, B. A. Bhuvaneswari, A. S. Guptha, and S. S, "CLNet: a contactless fingerprint spoof detection using deep neural networks with a transfer learning approach," *Multimedia Tools and Applications*, vol. 83, no. 9, pp. 27 703–27 722, 2024, doi: 10.1007/s11042-023-16511-6.

[5] J. Choi, K. J. Noh, S. W. Cho, S. H. Nam, M. Owais, and K. R. Park, "Modified Conditional Generative adversarial Network-Based Optical Blur Restoration for Finger-Vein Recognition," *IEEE Access*, vol. 8, pp. 16 281–16 301, 2020, doi: 10.1109/aCCESS.2020.2967771.

[6] B. Zhang, S. Zhao, L. Fei, and S. Li, "Innovative Hyperspectral Hand-Vein Recognition Systems," in *Advanced Hand-based Biometrics*. Singapore: Springer Nature Singapore, 2026, pp. 145–158, doi: 10.1007/978-981-95-0970-6_8.

[7] W. Nie, Z. Yuan, J. Hu, C. Li, Y. Wang, J. Feng, R. Wang, and X. Feng, "A Two-Phase Multispectral Dorsal Hand Vein Recognition Approach," in *2025 6th International Conference on Internet of Things, Artificial Intelligence and Mechanical Automation, IoTAIMA 2025*. IEEE, 2025, pp. 464–467, doi: 10.1109/IoTAIMA66468.2025.11212755.

[8] R. Mohammadzadeh, "Hardware-aware neural architecture search for quantized neural networks exploration on resource-constrained devices," Master's thesis, Ecole Polytechnique, Montreal (Canada), 2023.

[9] W. Yang, W. Luo, W. Kang, Z. Huang, and Q. Wu, "FVRAS-Net: An Embedded Finger-Vein Recognition and AntiSpoofing System Using a Unified CNN," *IEEE Transactions on Instrumentation and Measurement*, vol. 69, no. 11, pp. 8690–8701, 2020, doi: 10.1109/TIM.2020.3001410.

[10] S. E. Boudjellal, N.-E. Boukezzoula, and A. Boudjelal, "Hybrid convolutional transformer-based network model for finger vein identification," *Journal of Electronic Imaging*, vol. 32, no. 05, p. 53005, 2023, doi: 10.1117/1.jei.32.5.053005.

[11] I. Kouadra, M. Bouchra, T. Bekkouche, and L. Ziet, "Encryption face area in color images using Chaotic Maps," in *International Conference on Pioneer and Innovative Studies*, vol. 1, 2023, pp. 501–506, doi: 10.59287/icpis.880.

[12] M. Chen, C. Yuan, and Y. Lv, "Fingerprint liveness detection approaches: a survey," *International Journal of Autonomous and Adaptive Communications Systems*, vol. 16, no. 6, pp. 564–583, 2023, doi: 10.1504/IJAACS.2023.134830.

[13] S. A. Jakhete and N. Kulkarni, "DeepEmoNet: A Lightweight Context-Aware CNN for Multimodal Emotion Recognition," *Engineering, Technology and Applied Science Research*, vol. 16, no. 2, pp. 32 844–32 854, 2026, doi: 10.48084/etasr.15258.

[14] J. S. Tan, A. R. See, and A. B. Alcuitas, "A Comparative Study of Lightweight Convolutional Models for Visual Surface Material Classification," *IEEE Access*, vol. 14, pp. 66 179–66 186, 2026, doi: 10.1109/ACCESS.2026.3686791.

[15] S. M. J. Tahmid, W. K. Chowdhury, and N. Islam, "Multi-dataset plantar thermography integration for scalable deep learning-based early detection of diabetic foot ulcers," Ph.D. dissertation, Brac University, 2025.

[16] M. Tan and Q. V. Le, "EfficientNetV2: Smaller Models and Faster Training," in *Proceedings of Machine Learning Research*, vol. 139. PMLR, 2021, pp. 10 096–10 106.

[17] H. I. Liu, M. Galindo, H. Xie, L. K. Wong, H. H. Shuai, Y. H. Li, and W. H. Cheng, "Lightweight Deep Learning for Resource-Constrained Environments: A Survey," *ACM Computing Surveys*, vol. 56, no. 10, pp. 1–42, 2024, doi: 10.1145/3657282.

[18] T. H. C. Silva and R. A. R. Oliveira, "Lightweight AI Models in Mineral Processing: Classifying Hydrocyclone Underflow With ResNet-18 and MobileViT-V2," *IEEE Access*, vol. 13, pp. 122 556–122 567, 2025, doi: 10.1109/ACCESS.2025.3587227.

[19] W. Wu, A. Liu, J. Hu, Y. Mo, S. Xiang, P. Duan, and Q. Liang, "EUAVDet: An Efficient and Lightweight Object Detector for UAV Aerial Images with an Edge-Based Computing Platform," *Drones*, vol. 8, no. 6, p. 261, 2024, doi: 10.3390/drones8060261.

[20] A. Cherry, A. Nasser, W. Salameh, M. Abou Ali, and M. Hajj-Hassan, "Real-Time PPG-Based Biometric Identification: Advancing Security with 2D Gram Matrices and Deep Learning Models," *Sensors*, vol. 25, no. 1, p. 40, 2025, doi: 10.3390/s25010040.

[21] S. Chinta, "Edge AI for Real-Time Decision Making in IOT Networks," *International Journal of Innovative Research in Computer and Communication Engineering*, vol. 12, no. 09, pp. 11 293–11 309, 2024, doi: 10.15680/ijircce.2024.1209044.

[22] N. Miura, A. Nagasaka, and T. Miyatake, "Extraction of finger-vein patterns using maximum curvature points in image profiles," *IEICE Transactions on Information and Systems*, vol. E90-D, no. 8, pp. 1185–1194, 2007, doi: 10.1093/ietisy/e90-d.8.1185.

[23] I. Riaz, A. Nazri Ali, H. Ibrahim, and I. A. Huqqani, "Multimodal Biometric Recognition System Based on Feature-Level Fusion of Dorsal Finger Crease and Finger Knuckle Print," *IEEE Transactions on Artificial Intelligence*, vol. 7, no. 4, pp. 1904–1916, 2026, doi: 10.1109/TAI.2025.3563315.

[24] B. Hou, H. Zhang, and R. Yan, "Finger-vein biometric recognition: A review," *IEEE Transactions on Instrumentation and Measurement*, vol. 71, pp. 1–26, 2022.

[25] C. H. Hsia, L. Y. Ke, and S. T. Chen, "Improved Lightweight Convolutional Neural Network for Finger Vein Recognition System," *Bioengineering*, vol. 10, no. 8, p. 919, 2023, doi: 10.3390/bioengineering10080919.

[26] N. C. Tran, B. T. Pham, V. C. M. Chu, K. C. Li, P. T. Le, S. L. Chen, A. Z. K. Frisky, Y. H. Li, and J. C. Wang, "Zero-FVeinNet: Optimizing Finger Vein Recognition with Shallow CNNs and Zero-Shuffle Attention for Low-Computational Devices," *Electronics (Switzerland)*, vol. 13, no. 9, p. 1751, 2024, doi: 10.3390/electronics13091751.

[27] A. S. Alaerjan, A. M. Mostafa, A. A. Mahmoud, and M. Ezz, "Efficient multi-finger vein recognition using layer-wise progressive MobileNet fine-tuning and a Dense-Head Probabilistic Siamese Network," *Scientific Reports*, vol. 16, no. 1, 2026, doi: 10.1038/s41598-025-32132-5.

[28] Y. Wang, J. Gui, Y. Y. Tang, and J. T. Y. Kwok, "CFVNet: An End-to-End Cancelable Finger Vein Network for Recognition," *IEEE Transactions on Information Forensics and Security*, vol. 19, pp. 7810–7823, 2024, doi: 10.1109/TIFS.2024.3436528.

[29] Y. Li, G. Yuan, Y. Wen, J. Hu, G. Evangelidis, S. Tulyakov, Y. Wang, and J. Ren, "EfficientFormer: Vision Transformers at MobileNet Speed," *Advances in Neural Information Processing Systems*, vol. 35, pp. 12 934–12 949, 2022, doi: 10.52202/068431-0940.

[30] C. Gu, J. Yu, and C. Zhang, "Learning disentangled representations for controllable human motion prediction," *Pattern Recognition*, vol. 146, p. 109998, 2024, doi: 10.1016/j.patcog.2023.109998.

[31] B. A. El-Rahiem, F. E. El-Samie, and M. Amin, "Multimodal biometric authentication based on deep fusion of electrocardiogram (ECG) and finger vein," *Multimedia Systems*, vol. 28, no. 4, pp. 1325–1337, 2022, doi: 10.1007/s00530-021-00810-9.

[32] K. J. Noh, J. Choi, J. S. Hong, and K. R. Park, "Finger-vein recognition using heterogeneous databases by domain adaption based on a cycle-consistent adversarial network," *Sensors (Switzerland)*, vol. 21, no. 2, pp. 1–28, 2021, doi: 10.3390/s21020524.

[33] Y. Tang, K. Han, J. Guo, C. Xu, C. Xu, and Y. Wang, "GhostNetV2: Enhance Cheap Operation with Long-Range Attention," *Advances in Neural Information Processing Systems*, vol. 35, pp. 9969–9982, 2022, doi: 10.52202/068431-0724.

[34] C. Kuraku, "Biometric Authentication In Digital Payments: Utilizing AI And Big Data For Real-Time Security And Efficiency," *Educational Administration: Theory and Practice*, vol. 26, no. 4, pp. 954–964, 2024, doi: 10.53555/kuey.v26i4.7590.

[35] D. Ngo, H. C. Park, and B. Kang, "Edge Intelligence: A Review of Deep Neural Network Inference in Resource-Limited Environments," *Electronics (Switzerland)*, vol. 14, no. 12, p. 2495, 2025, doi: 10.3390/electronics14122495.

[36] L. Lin, Y. Zhao, J. Meng, and Q. Zhao, "A Federated Attention-Based Multimodal Biometric Recognition Approach in IoT," *Sensors*, vol. 23, no. 13, p. 6006, 2023, doi: 10.3390/s23136006.

[37] J. Zhang, X. Liu, S. Zheng, W. Zhang, and J. Gu, "Dual-Field Microvascular Segmentation: Hemodynamically-Consistent Attention Learning for Retinal Vasculature Mapping," *IEEE Journal of Biomedical and Health Informatics*, vol. 30, no. 6, pp. 5142–5155, 2026, doi: 10.1109/JBHI.2025.3634356.

[38] N. Y. Abdullah and S. A. Alkazzaz, "Physical Exercise Classification Using MobileNet," in *Lecture Notes in Networks and Systems*, vol. 1295. Springer Nature Singapore, 2025, pp. 223–234, doi: 10.1007/978-981-96-3311-1_18.

[39] M. S. M. Asaari, S. A. Suandi, and B. A. Rosdi, "Fusion of Band Limited Phase only Correlation and Width Centroid Contour Distance for finger based biometrics," *Expert Systems with Applications*, vol. 41, no. 7, pp. 3367–3382, 2014, doi: 10.1016/j.eswa.2013.11.033.

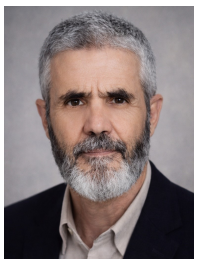
[40] Y. Lu, S. J. Xie, S. Yoon, Z. Wang, and D. S. Park, "An available database for the research of finger vein recognition," in *Proceedings of the 2013 6th International Congress on Image and Signal Processing, CISP 2013*, vol. 1. IEEE, 2013, pp. 410–415, doi:

10.1109/CISP.2013.6744030.
[41] H. H. Aghdam and E. J. Heravi, *Guide to Convolutional Neural Networks*. New York, NY: Springer, 2017, doi: 10.1007/978-3-319-57550-6.
[42] Z. Zhang and M. R. Sabuncu, "Generalized cross entropy loss for training deep neural networks with noisy labels," *Advances in Neural Information Processing Systems*, vol. 2018-December, pp. 8778–8788, 2018.
[43] D. P. Kingma and J. L. Ba, "Adam: A method for stochastic optimization," *3rd International Conference on Learning Representations, ICLR 2015 - Conference Track Proceedings*, 2015.
[44] Y. S. Tahir and B. A. Rosdi, "FV-EffResNet: an efficient lightweight convolutional neural network for finger vein recognition," *PeerJ Computer Science*, vol. 10, p. e1837, 2024, doi: 10.7717/peerj-cs.1837.
[45] Z. Zhang and M. Wang, "Finger vein recognition based on lightweight convolutional attention model," *IET Image Processing*, vol. 17, no. 6, pp. 1864–1873, 2023, doi: 10.1049/ipr2.12761.
[46] Z. Zhang, P. Liu, C. Su, and S. Tong, "A High-Speed Finger Vein Recognition Network with Multi-Scale Convolutional Attention," *Applied Sciences (Switzerland)*, vol. 15, no. 5, p. 2698, 2025, doi: 10.3390/app15052698.
[47] N. Devkota and B. W. Kim, "Finger Vein Recognition Using DenseNet with a Channel Attention Mechanism and Hybrid Pooling," *Electronics (Switzerland)*, vol. 13, no. 3, p. 501, 2024, doi: 10.3390/electronics13030501.
[48] T. Liu, J. Li, J. Wu, B. Du, J. Wan, and J. Chang, "Confusable facial expression recognition with geometry-aware conditional network," *Pattern Recognition*, vol. 148, p. 110174, 2024, doi: 10.1016/j.patcog.2023.110174.
[49] K. Jha and A. Jain, "Tiny-transformer based multimodal biometric authentication with edge fusion and federated split learning," *Signal, Image and Video Processing*, vol. 20, no. 8, p. 469, 2026, doi: 10.1007/s11760-026-05521-0.
[50] K. K. Prakasha and U. Sumalatha, "Privacy-Preserving Techniques in Biometric Systems: Approaches and Challenges," *IEEE Access*, vol. 13, pp. 32 584–32 616, 2025, doi: 10.1109/ACCESS.2025.3541649.

BIOGRAPHIES OF AUTHORS



Abdelhalim Hazzem received the B.Eng. degree in Electrical Engineering from Ferhat Abbas University Setif 1, Setif, Algeria, in 2011, and the M.Sc. degree in Embedded Systems Electronics from the same university in 2016. He is currently pursuing the Ph.D. degree in Electrical Engineering at Ferhat Abbas University Setif 1, Setif, Algeria, since 2020. He is a member of the Power Electronics and Industrial Control Laboratory (LEPCI), Department of Electrical Engineering, Ferhat Abbas University Setif 1. His current research interests include power electronics, embedded systems, renewable energy systems, industrial control, intelligent control, optimization techniques, and electric drives. He can be contacted at email: abdelhalim.hazzem@univ-setif.dz.



Lahcene Ziet received the Bachelor's, Master's (Magistére), and Ph.D. degrees in Electronics from the University of Sétif, Algeria, in 1990, 1994, and 2007, respectively. He is currently an Associate Professor with the Department of Electronics, University of Sétif. Since joining the University of Sétif, in 1993, he has contributed to numerous academic and research initiatives, mentoring students and participating in international collaborations. He has been actively involved in advancing the fields of embedded systems and security technologies. He has authored or co-authored several articles published in reputable journals and conferences in his research areas. His research interests include biometrics, cryptography, and the implementation of embedded FPGA accelerators. He can be contacted at email: lahcene.ziet@univ-setif.dz.



Imane Kouadra received the Bachelor's and Master's degrees in Network and Telecommunications from the Department of Electronics, Faculty of Technology, Ferhat Abbas University, Setif, Algeria, in 2021. She is currently pursuing the Ph.D. degree specializing in Telecommunications Networks with Ferhat Abbas University. She is an adjunct instructor with the voice over internet protocol (VoIP) module. Her research interests include digital image and signal processing, cryptography, biometric security, data mining, pattern recognition, machine learning, deep learning, and cybersecurity. She can be contacted at email: imane.kouadra@univ-setif.dz.



Abd-ettouab Manallah he received his Bachelor's degree in Electronics from Ferhat Abbas University, Sétif-1, Algeria, in 2023, and his Master's degree in Embedded Systems Electronics from the same university in 2025. He is currently working as a quality control inspector at Condor Multimedia. His research interests focus on artificial intelligence and biometrics.He can be contacted at email: abdettouabmanallah@gmail.com.



Anfal Rouabhi received her Bachelor's degree in Electronics from Ferhat Abbas University, Sétif, Algeria, in 2023, and her Master's degree in Embedded Systems Electronics from the same university in 2025. She is currently working as a quality control inspector at Condor Multimedia. Her research interests include artificial intelligence and biometrics.She can be contacted at email: anfalrouabhi96@gmail.com.



Tewfik Bekkouche received the Engineering and Ph.D. degrees in Electronics in 1990 and 2018, respectively. He is currently a Professor at the University of Bordj Bou Arreridj, Algeria. With a solid academic background and extensive expertise in the field, he is committed to developing secure and innovative solutions in information technology. His research interests include image encryption, biometrics, and information security. He can be contacted at email: toufik.bekkouche@univ-setif.dz.